

Superfluidic nature of self-driven nanofluidics at liquid-gas interfaces

Vinitha Johny^{1,2}, Sonia Antoranz Contera³, and Siddharth Ghosh^{1,2,4*}

¹*International Center for Nanodevices, Center for Nano Science and Engineering, Indian Institute of Science, Bangalore.*

²*Department of Science, Open Academic Research Council, Kolkata,
India & Department of Science, Open Academic Research UK CIC, Cambridge, UK.*

³*Department of Physics, University of Oxford, UK.*

⁴*Department of Applied Mathematics and Theoretical Physics, University of Cambridge, UK.*

The focus of this paper is to study the non-linear dynamics of confined nanopore system at liquid-air interface. We are seeking fundamental explanations to the unexpected observations happening at this confined scale. The finite range interactions in position space between the interacting species are quantified with corresponding critical velocity of the system, which leads to the occurrence of Bose-Einstein condensate within the liquid phase. This is visualised using finite element method and analysed mathematically with Landau criterion. The condensates are formed as a consequence of the nanofluidic transport through pores on a 100 nm thick solid interface. The simulations shows that the systems having more than one nanopore with sub-100 nm diameter are highly non-linear and complex. The approximation of relevant classical systems to existing quantum systems divulge new results and corrections at a fundamental level. The formation of oscillating condensate within the system in the liquid phase have been resolved along with crucial observations in the system, which was left unknown in our prior study. The high velocity near the specific boundaries of the system, the sudden disappearance of oscillations and its dependence on evaporation are explored in light of existing fundamental researches in nanoscale domain.

Structure: superfluidity, quantum confinement, quantum nanofluidics, nanopores, liquid-gas interface

I. INTRODUCTION

The integrability of a physical system having classical observable to a canonically quantised system do not have a clear explanation even today [1, 2]. A reason behind this is that not all quantum parameters, such as spin has its own classical counterpart [3]. A quantum mechanical system is defined by the measurement of complete set of commuting observable and specific operators; such system can have impeccable correlation to the classical observable. An example of this system with classical phase-space functions could be a fluid reservoir separated by a solid interface, which creates two separate volume fractions of air and water as depicted in Figure 1a. These fluidic systems allows mixing of the fluids through certain nanometric pores on the solid interface. Dynamics of such systems with a single pore on the interface has already been addressed previously by us [4] where the dynamics of multipore systems was unclear due to pure classical treatment. In this paper, we present the dynamics of multipore nanofluidic systems by following a necessary transition from classical to quantum approximations.

II. COMPLEX SELF-DRIVEN NANOFLUIDICS

The physics of nanofluidics can be empirically divided into two parts — below and above 100 nm. The sub-100 nm regimes with quasi-quantum-classical approaches

are quite demanding. However, in room temperature – water-air (liquid-gas) interface is crucial for the transpiration process in trees and, flow dynamics from such a system in classical frame of reference has significantly clear similarities to specific quantum dynamics of the same system by numerical and theoretical analysis. Let us explore the interfacial behaviour and existence of the phases of matter inside sub-100 nm fluidic channel (where length of reservoir is much larger than the diameter of the pore) undergoing a strong differential pressure. The flow dynamics of such systems generally falls under conventional laminar flow regime. However, the trajectories of velocity streamlines in Figure 1b shows significant deviation from this expectation.

The coexistence of coupled anharmonic and harmonic components in the denser volume fraction as shown in Figure 1b will require us to use quantum mechanical approach to define its dynamics completely. One of the critical parameters that could cause simultaneous existence of two different flow velocities in the system without any external forces can be temperature. The peculiarities of dynamics exhibited by liquid 4-He under the lambda temperature (≈ 2.17 K) is well known as superfluidity [5]. In the non-perfect BEC, the repulsive and attractive forces in the system influence superfluidity [6]. This is also possible in case of nonequilibrium real liquids subjected to specific operating conditions. The coherence length of liquid 4-He diverges at the transition point and attains a steady state at 0.1 nm due to quantum coherence [7]. In such a system, the condensate moves with a very small relative velocity without any external forces which leads to the presence of super fluidity in the system. London [8] considered liquid 4-He subjected to a pressure change to exist in dual nature. The coexistence of this dual na-

* Email of correspondence: sg915@cam.ac.uk

ture with one is being dependent on temperature in a conventional manner, and other is not being condensed even below its vapour pressure in the lowest energy state.

Hence, in the temperature range towards Lambda point the coefficient of viscosity changes from 1×10^{-5} CGS units to 3×10^{-5} CGS units for harmonic component and nearly 0 for an-harmonic or superfluidic component [8]. This is due to the anomalies in the momentum distribution function within the particles. This impediment in a confined system at the nanometric domain is potentially due to friction induced by the walls or particle movement. The ability to observe explicit quantum mechanical phenomenon in room temperature water, as in a pure quantum 4-He liquid inside nanopores is also crucial in quantum optomechanics [9] FEM analysis demonstrate the velocity vortices oscillating within the water phase, while the high velocity normal component is pushed towards the confined walls. This highly anisotropic behaviour of velocity flow trajectories (connecting 10 equidistant seed points in water phase) as shown in Figure 1c along each degree of freedom, makes it complex to be validated completely using non-linear Schrödinger equation. Hence, In this paper we use the Landau criterion to validate the criterion for superfluidity.

III. TOWARDS QUANTUM NANO FLUIDICS AT ROOM-TEMPERATURE.

The creation of improvised nanofluidic devices are continually looking for intrinsic explanations for observations occurring on confined systems at nanometer scale and the solutions are most likely to occur in the quantum realm.

Until the emergence of quantum thermodynamics, where we try to explain such systems using the potential of current quantum systems, some complicated phenomena at this scale were difficult to be placed merely as quantum or thermodynamic system. One such example is a qubit system with two dimensional Hilbert space which was analysed and compared by its classical and quantum counterparts [10]. This was done by the approximation technique by Lukin et al. [11].

Nevertheless, a confined sub 100 nm multi-pore system exhibiting thermodynamic behaviour may seem to be solved as a classical system but its complexity and turbulent behaviour demands it to be qualitatively analysed in the quantum realm. As researches have already been able to interpret and measure the super fluidity in nanochannels, the observations in this paper evokes the possibility of superfluidity in confined nanosystems. Rojas et al. [7] studied the dynamics of super-fluid 4-He, coupled with super fluid Helmholtz resonance by developing a nanomechanical resonator which showed unexpected quantum turbulence. This is due to increased dissipation within the system. In a 9 nL system, the superfluidic mass was estimated to be approximately 24 ng

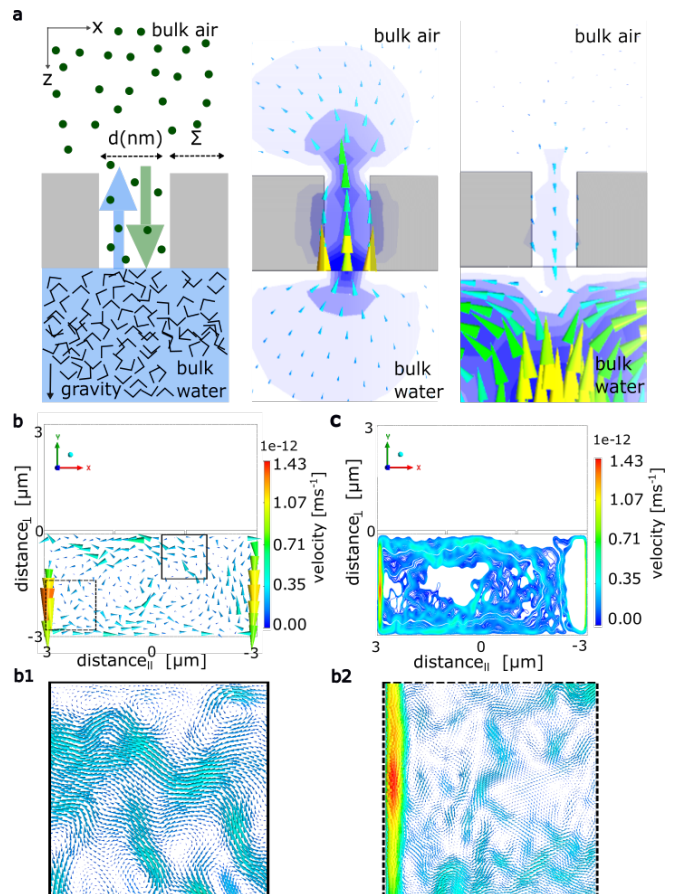


FIG. 1. (a) Overview of the phase exchange through a nanopore, and the possible along with the flow vector orientation of particles in the system. (b) The velocity vectors distribution along the resultant swirls created within the water phase when no phase exchange occurs, ($d = 100$ nm situated at $\sigma = 2000$ nm, 4000 nm). (b1, b2) Evident image of the randomness of vortices and swirls formed within a small area near the nanopore and near the walls inside liquid phase. (c) Velocity streamlines connecting 10 equidistant sample points with system.

at $(T - T_\lambda) = 2$ mK and 960 ng at near 1.6 K where T_λ is the temperature at the lambda point. In a confined system of 2 different phases separated by an interfacial nanochannel, below a critical velocity the particles acts as 2 different clusters with independent physical properties. The normal particles with higher velocity were moved towards the wall while the relatively slower superfluidic particles were dragged away from the boundaries of the confined system with respect to the reference velocity (reference velocity = 4.2×10^{-9} m/s). In the nanosystem developed by Rojas et al. [7], for frequency range below 5 KHz the critical velocity was found to be $1 \mu\text{m}$, which confirms the oscillation of superfluidic components in the channels and the adherence of normal components towards the walls. Having said so, the physics behind the interaction happening in such systems is still unclear and needs to be determined. Figure 1(b1, b2) gives a clear

picture on the compexity of the transport along with velocity vectors.

IV. ANALYTICAL APPROACH

Consider the liquid phase in Figure 1b, where the vortices are observed in the form of velocity vectors. The vectors are highly turbulent and has varying orientation to different locations within the phase. We are primarily interested in solving the cause of these vortices. The reference velocity is set to 4.2×10^{-9} m/s and hence the observed velocity variations in Figure 1a are very significant. The velocity vector magnitude near to the nanopore is significantly lower (0.35×10^{-12} m/s) than those near the walls. Hence, it is projected separately as in Figure 1b1 and Figure 1b2 for clear understanding. Figure 1c shows the velocity streamlines connecting 10 equally distant sample points within the water phase. These seed points are randomly distributed but are equidistant to each other to represent an overall motion of the particles in the liquid phase. It is evident that the particle velocity near to the boundary is greater (1.43×10^{-12} m/s) than the velocity at the center part of the liquid phase. This may occur due to the coexistence of normal, and superfluidic components in the system. By normal particles we mean those particles which exhibits conventional thermodynamic behavior. Since the pressure near the nanopore at the interface is too high, the liquid-air phase transition occurs indicating the rise of temperature in the system. Hence, if the velocity at the walls are greater than the Landau critical velocity, there is a possibility of coupling between harmonic components and anharmonic components in the $6 \mu\text{m} \times 3 \mu\text{m}$ liquid phase region (as per weak interaction of Bose gases). Then, this can be the visualization of the mathematical abstraction of the phenomenon of vortices in BEC. In our previous work [4], a reverse flow was observed in certain nanocavities which suggest the direction of momentum in the opposite direction of actual flow. This is Landau criterion for energetically unstable superfluidity.

At this point of our study in Figure 1a, we assume a finite range interaction of $\zeta(\mathbf{r}_0 - \mathbf{r}_1)$ in position space. Then the critical velocity \mathbf{v}_c is given by [12]

$$\mathbf{v}_c = \left[\left(\frac{\mathbf{p}_c}{2m} \right)^2 + \frac{\rho \zeta_\tau}{m} \right]^{1/2} \quad (1)$$

where \mathbf{p}_c is the critical momentum, m is the mass of the particle, ρ is the density, ζ_τ is $\zeta(\tau \mathbf{p}_c)$ where, τ is any integer and $\zeta(\mathbf{p})$ is the Fourier transform of $\zeta(\mathbf{r}_0)$. When the phase velocity and group velocity of particles becomes equal, the velocity near the walls or boundary is expected to be greater than the critical velocity. For the condensate momentum \mathbf{q} ,

$$\mathbf{q}^2 > \mathbf{p}_c^2/4 + m\rho\zeta_1 \quad (2)$$

where ζ_1 represents the scenario where $\tau = 1$. In system as shown in Figure 1b, five equidistant parallel and perpendicular lines with respect to the orientation of nanopore are plotted within the water phase geometry. Again, 10 equidistant data points are considered along each of these lines and their velocity variations are recorded as shown in Figure 2(a-f) to check the convergence of the solution to the criterion in equation 2. In Figure 2a1, the velocity magnitudes of the data points corresponding to the parallel lines to the orientation of nanopore in the order of their distribution through the geometry in two pore system ($d = 30$ nm situated at $\sigma = 2000$ nm, 4000 nm) is shown. The data points on the line near to the boundary marks the highest velocity of 2×10^{-12} m/s in the system. In Figure 2a2, the velocity magnitudes of the data points corresponding to the perpendicular lines to the orientation of nanopore in the order of their distribution through the geometry in two pore system ($d = 30$ nm situated at $\sigma = 2000$ nm, 4000 nm) is given. Here, the data points in the air phase drops down to zero and only the 2 lines in the water phase shows evident deviation in flow vectors. In Figure 2b1, the velocity magnitudes of the data points corresponding to the parallel lines to the orientation of nanopore in the order of their distribution through the geometry in three pore system ($d = 30$ nm situated at $\sigma = 2000$ nm, 4000 nm) is shown. Here, the flow vectors are prominent towards the center also, apart from boundary. But the maximum velocity magnitude in the system has now reduced to 1×10^{-12} m/s. In Figure 2b2, the velocity magnitudes of the data points corresponding to the perpendicular lines to the orientation of nanopore in the order of their distribution through the geometry in three pore system ($d = 30$ nm situated at $\sigma = 2000$ nm, 4000 nm) is given. In Figure 2c1, the velocity magnitudes of the data points corresponding to the parallel lines to the orientation of nanopore in the order of their distribution through the geometry in four pore system ($d = 30$ nm situated at $\sigma = 2000$ nm, 4000 nm) is shown. Unlike the two pore, and three pore systems of $d = 30$ nm case, the velocity magnitude has variations in the water phase also. Here, there is flow through the nanopore which makes significant changes in air phase also in terms of flow vectors. The highest flow magnitude is observed through the nanopore and has magnitude of 1.6×10^{-12} m/s. In Figure 2c2, there is significant variations in velocity components corresponding each data points. Now, we change the pore size from 30 nm to 70 nm. Figure 2 d1 shows the flow velocity corresponding to the data points on the lines, parallel to the orientation of nanopore in $d= 70$ nm two pore system. The maximum velocity corresponds to 1.4×10^{-12} m/s and is observed near the boundary. In Figure 2d2 the maximum velocity of 1×10^{-12} m/s is observed at the data point located inside one of the pore. Figure 2e1 shows the flow velocity corresponding to the data points on the lines, parallel to the orientation of nanopore in $d= 70$ nm three pore system. In Figure 2e2, velocity of 5×10^{-13} m/s is the

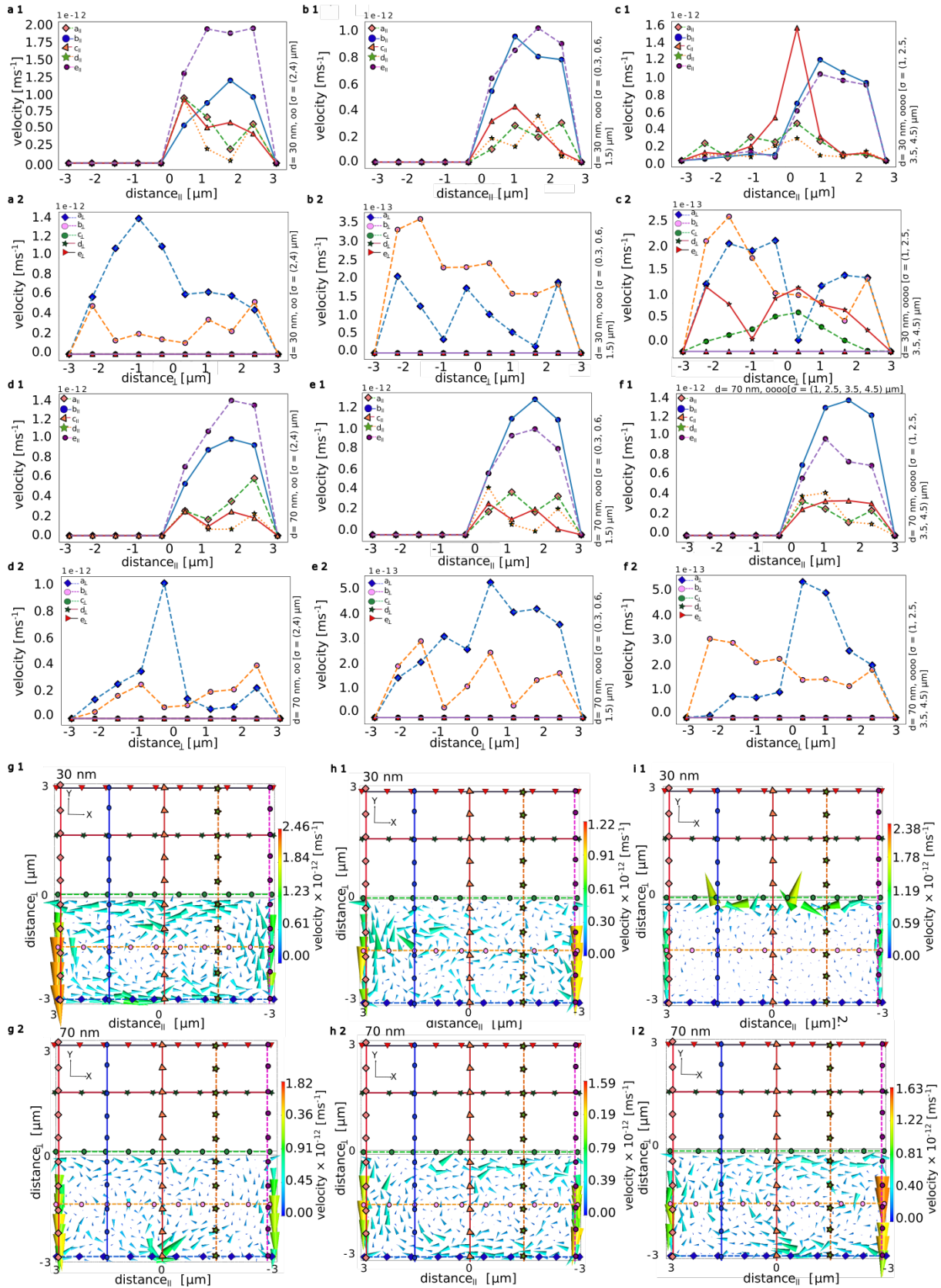


FIG. 2. Variation in particle velocity along the orientation of nanopore throat ($distance_{||}$), and perpendicular to the orientation of nanopore throat ($distance_{\perp}$). (a1, b1, c1) Velocity variations along $distance_{||}$ for systems with two, three, four nanopores respectively for $d = 30$ nm. (a2, b2, c2) Velocity variations along $distance_{\perp}$ for systems with two, three, four nanopores respectively for $d = 30$ nm. (d1, e1, f1) Velocity variations along $distance_{||}$ for systems with two, three, four nanopores respectively for $d = 70$ nm. (d2, e2, f2) Velocity variations along $distance_{\perp}$ for systems with two, three, four nanopores respectively for $d = 70$ nm. (g1, h1, i1) Vector orientation of particle velocity for systems having two, three, four nanopores respectively for $d = 30$ nm. (g2, h2, i2) Vector orientation of particle velocity for systems having two, three, four nanopores respectively for $d = 70$ nm.

highest of all the lines perpendicular to the orientation of nanopore in three pore system with $d=70$ nm. Now, the critical velocity is taken to be the velocity of the system at which highest number of data points converges regardless of change in pore size d . Now, let us try to unfold our understanding on such systems in quantum realm.

V. OUTLOOK — QUANTUM STATISTICAL APPROACH

Let us start from the Feynman approach towards phase transition. At transition temperature, consider liquid H_2O in a nanochannel. H_2O , being a non linear triatomic molecule with three modes of vibrations has a frequency range between 3652 cm^{-1} and 3756 cm^{-1} and changes its dipole during the vibrations. The matter waves associated with it has velocity v and the wavelength λ is defined as $\lambda = h/p$.

$$E = \sqrt{\mathbf{p}^2 c^2 + E_0^2} \quad (3)$$

$$\lambda = \frac{hc}{\sqrt{k_e^2 + 2k_e E_0}} \quad (4)$$

where $E = k_e + E_0$, E_0 is the rest mass energy, \mathbf{p} is the momentum, and k_e is the kinetic energy of the particle. Consider two waves y_1 and y_2 super imposing constructively such as $\mathbf{y} = \mathbf{y}_1 + \mathbf{y}_2$. then,

$$\mathbf{y} = B[\cos(\omega_1 t - k_1 x) + \cos(\omega_2 t - k_2 x)] \quad (5)$$

$$\mathbf{y} = 2B[\cos(\Delta\omega t - \Delta k x) + \cos(\omega t - k x)] \quad (6)$$

where $(\Delta\omega t - \Delta k x)$ is the modulation in amplitude due to group velocity and $(\omega t - k x)$ is the modulation of amplitude due to phase velocity, $k = 2\pi/\lambda$, ω is the angular frequency of the wave. In quantum physics, the velocity of particle is referred to its group velocity and hence in a system of particles with different group velocities, the rate of difference in phases can determine the rate of superfluidity in the system with respect to its reference velocity. Their velocities will be out of phase at the zone boundaries and in the center by which the initial coherent state of the particles are disturbed. It is expected that when the minimum velocity in our system becomes equal to the Landau critical velocity, the phase velocity becomes equal to the group velocity[12].

$$\mathbf{v}_g = \mathbf{v}_p + k(d\mathbf{v}_p/dk) \quad (7)$$

which leads to the dispersion relation,

$$\mathbf{v}_g = \mathbf{v}_p - \lambda(d\mathbf{v}_p/d\lambda) \quad (8)$$

This relates to the energy exchange within the strong and weak coupling which is applicable at the quantum-classical boundaries of the system [13]. Lukin, in his

work on ultra slow single photons showed that one among two weak waves of energy $h\nu$ can modify the properties of one component wave resulting in a phase shift [14]. The quantum entanglement thus formed causes super positions and quantum interference. A mathematical model to understand such non linear quantum systems was done by [15]. In his work, he considered the nonlinear Schrödinger Gross-Pitaevskii equation to understand the quantum dynamics of a cubical system, where the maximum particle interaction scale is the length of the system. At this point, it is vital to determine if the system is in equilibrium or whether the observation has a probability of decaying over time. The nonlinear dispersive effects on the wave vector cancel out the steepening effect of waves in linear approximation, and the system achieves an equilibrium state, according to Tsuzuki[16]. In such a system, where the ground state scattering length has a strong dependence on the repulsive interactions, Gross-Pitaevskii equation could pave light to the dynamics of the particles within the system.

This may be complex problem due to the highly anisotropic nature of the particles along each axis, and would create a quantum confinement of many body system.

Let us start with the identity of the particles in the 2D continuum of states in the system. For the particles to obey BEC, they should obey the Bose Einstein statistics, What if these particles are Fermions?—As non-Hermitian superfluidity is also a possibility here. The answer to this question lies in the observed vortex pairs of the system which shows that these particles are of type-1 bosons as in [17]. As 4-He atom which is considered to be of such kind, bound pair of spin half particles as seen in [4] can be considered to have characteristics as that of bosons. Hence we begin our journey with the method of second quantization in the context of Quantum field theory. As it defines many body operators which are crucial in superconductivity and superfluidity [18] in terms of creation and annihilation operators. We are aware of the switching mechanism happening in the system which is unclear in the classical domain. Let us try to explain the system in this context, as every measurements are associated with creation and annihilation operators [19]. If the system has N number of single particle state $|\phi_b\rangle$ (orthonormal and complete, b is the index associated with all the quantum numbers), the action of creation operator creates a particle in the single particle state and if already a particle is present, then the effective action of the operator becomes zero. As for an annihilation operator, if a particle is present in a single particle state, it annihilates it. and if the state is already empty, there is no effective action. Then the scattering of a particle from state $|\phi_b\rangle$ to $|\phi_\chi\rangle$ is due to the annihilation operator followed by creation in state $|\phi_\chi\rangle$. This justifies to the dispersion relation from equation 8. The Hamiltonian of such system can be given as

$$H_0 = \sum_{b\chi} \langle \phi_\chi | h | \phi_b \rangle \varphi_\chi^\dagger \varphi_b \quad (9)$$

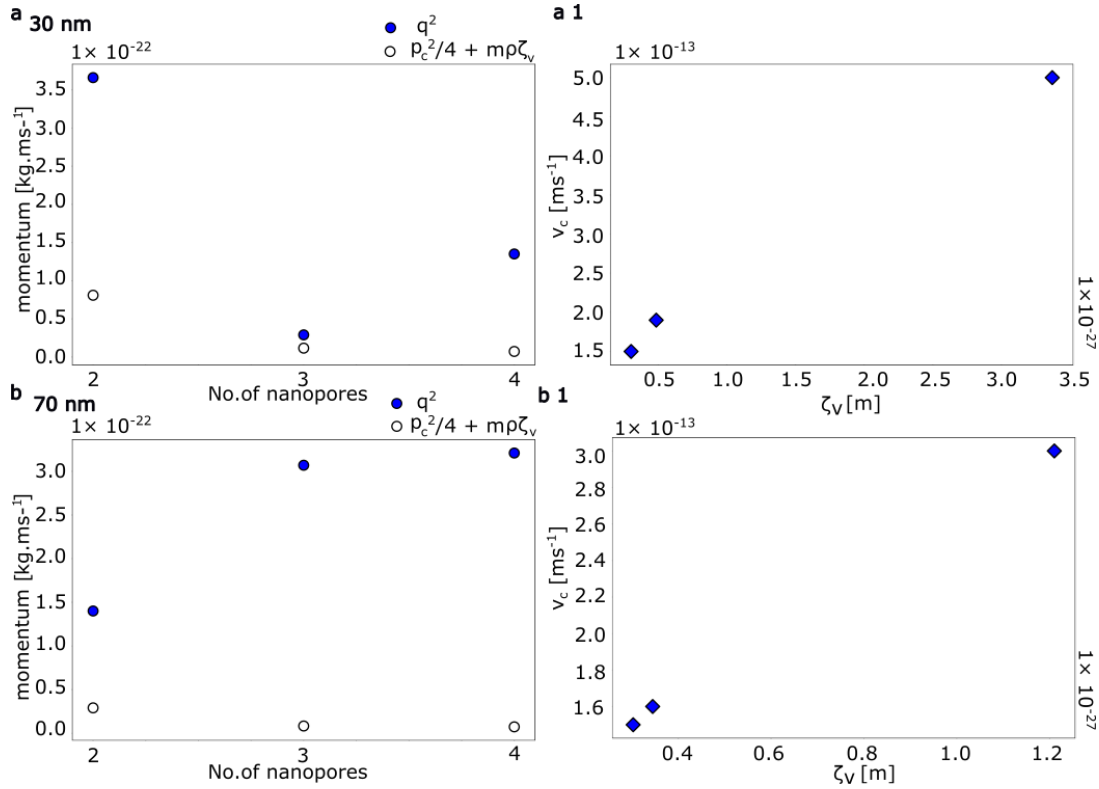


FIG. 3. Analytical validation of the Landau criterion in 30 nm and 70 nm nanopore systems and the dependency of finite range interaction with critical velocity. (a) Validation of the Landau criterion for $d = 30$ nm. (b) Validation of Landau criterion for $d = 70$ nm. (a1) Change in critical velocity of a system with the increase in finite range interaction in position space for $d = 30$ nm. (b1) Change in critical velocity of a system with the increase in finite range interaction in position space for $d = 70$ nm.

such that $h(i)$ is an operator dependent on the space coordinates of the particle [20]. where φ^\dagger is the creation operator and φ is the annihilation operator. Consider the basis state associated with spin Υ and wave number k , the kinetic energy of the system can be expressed as,

$$K_e = \sum_{i=1}^N \left(\frac{-\hbar^2}{2m} \right) \nabla_i^2 \quad (10)$$

$$\phi_{k\Upsilon}(r) = \langle r | k\Upsilon \rangle = \frac{1}{\sqrt{V}} \exp(ikr) | \Upsilon \rangle \quad (11)$$

where in 2D confinement, $k_x, k_y = 0, \pm \frac{2\pi}{L}, \pm \frac{4\pi}{L} \dots$

$$K_e = \sum_{k\Upsilon} \sum_{k^1\Upsilon^1} \langle k^1\Upsilon^1 | \frac{-\hbar^2}{2m} \nabla^2 | k\Upsilon \rangle \varphi_{k^1\Upsilon^1}^\dagger \varphi_{k\Upsilon}$$

$$K_e = (\hbar^2 k^2 / 2m) \varphi_{k\Upsilon}^\dagger \varphi_{k\Upsilon}$$

As confirmed from the analytical approach, as the delta function can express the particle number density at a position which is closely associated with the creation-annihilation operators. But this is not adequate to give

the number of particles in the system. Even though there are no significant physical changes in both air-water phases, particle exchange and energy exchange are evident enough to consider it as a member of the grand canonical ensemble. Then the ensemble average of total number of particles is obtained as the Bose-Einstein quantum distribution function ($n_i = \frac{1}{\exp \beta(\epsilon_i - Q) - 1}$), where Q is the chemical potential of the system, $\beta = \frac{1}{kT}$, ϵ_i is the energy state corresponding to the coordinate i .

VI. DISCUSSION

The observed highly anisotropic and non linear behaviour of particles for a laminar Reynolds number would be a tedious problem to encounter. For convenience, we plotted the velocity variation along parallel and perpendicular lines along the orientation of the nanopores as illustrated in figure.2. Systems having $d = 30$ nm, and $d = 70$ nm were simulated using ANSYS FLUENT 2021 R1 version, where d is the nanopore width. For each d , pore systems with two, three, and four nanopores were simulated separately to resolve their dynamics more efficiently and precisely. Fig 2a1, figure 2b 1, figure 2c 1 shows the velocity variations over the seed points in systems having 2, 3, 4 nanopores respectively for $d = 30$

nm.

Similarly, Figure 2d1, Figure 2e1, Figure 2f1 shows the velocity variations over the seed points in systems having 2, 3, 4 nanopores respectively for $d = 70$ nm. Even though the orientation and direction of the velocity vectors of these systems are random and non-linear (Figure 2(g - i)), most of the individual data points has a velocity near to $0.2 \times 10^{-12} \text{ ms}^{-1}$ regardless of their position which was considered to be the critical velocity. The system with most transport through the nanopore was the system with $d = 30$ nm and hence there were no vortices within the water phase and shows relatively high deviation in velocity profile (figure 2 c 1). This indicates the presence of transport through the nanopore and the absence of oscillating condensate within the water phase due to phase transition and diffusion. In all other systems, the velocity of line $c_{||}$ which indicates the flow through the nanopore was significantly lower, implying that there was very less flow to the air domain, which supports the objective of this study. Extreme flow velocity may clearly be seen at the container's extreme opposing ends, which are marked by lines $b_{||}$, $e_{||}$. The velocity tends to be similar as you get closer to the centre of the liquid domain, where the vortexes develop. According to the Landau criterion of superfluidity, the phase velocity becomes equal to the group velocity at the critical velocity and, the 9th sample point of most of the a harmonic components has a velocity of $2.4 \times 10^{-12} \text{ m/s}$ regardless of its position. Now, it is evident that the total number of particles within the water phase can be divided into two groups based on their velocity, location and the amount of turbulent characteristics they exhibit. The relatively low velocity components are an harmonic in nature and forms the condensate, which oscillates within the confinement of the container. These oscillations are again dependent on the forces of interaction within the interacting range and also coupled with the system's normal harmonic components that are pushed against the walls. In general for $d = 30$ nm and $d = 70$ nm, the square of the condensate momentum were higher than $\frac{p_c^2}{4} + m\rho\zeta\tau$ for all two, three, four, pore systems respectively as shown in fig 3a and fig 3b. These results lead us to the objective of this paper with the possibility of further investigation in such systems theoretically and through real time experimentation. The graphs in fig.3c and fig 3d reveals a lot about critical velocity's behaviour as the physical state of the system changes. It also has a linear relationship with the number of pores in the system and, it is highly dependent on the surface to area ratio within the interaction range.

ACKNOWLEDGMENTS

The authors thank Honeywell CSR fund awarded to thank International Center for Nano Devices for this research. SG thanks the German Research Foundation and Isaac Newton Trust for funding his research. The authors also thank Professor Natalia Berloff for many productive discussions.

VII. NOTATIONS

B	Wave amplitude
d	Diameter of the Nanopore
E	Energy
η	Viscosity of liquid
ϵ_i	Quantum mechanical energy state corresponding to the coordinate i
γ	Phase volume fraction in the multiphase flow
Γ	Cross sectional area
$h(i)$	Quantum mechanical operator
H_o	Hamiltonian of the system
κ	Phase variable
k	Wave number
k_B	Boltzmann constant
L	Flow length of instability
M	Mass transport through the nanopore
N	Total number of particles in the system
P	Pressure
p_c	Critical momentum
q	Condensate momentum
r	Radius of nanofluidic pore
ρ	Phase density
\mathbf{r}	Position vector
σ	Position of nanopore from the reference edge
τ	Constant corresponding to equation 1
v_p	Phase velocity
v_g	Group velocity
v_c	Critical velocity
W	Energy corresponding to work function of evaporation
ζ	Finite range interactions between particles
ϕ_b	Quantum state of system before interaction
ϕ_x	Quantum state of system after interaction
φ^\dagger	Creation operator
φ	Annihilation operator
Υ	Spin
K_e	Kinetic energy of the quantum system
Q	Chemical potential

- [1] J. Hietarinta, Quantum integrability is not a trivial consequence of classical integrability, *Physics Letters A* **93**, 55 (1982).
 [2] M. Medvidović and G. Carleo, Classical variational sim-

- ulation of the quantum approximate optimization algorithm, *npj Quantum Information* **7**, 1 (2021).
 [3] R. Graham and M. Höhnerbach, Two-state system coupled to a boson mode: quantum dynamics and classical

- approximations, *Zeitschrift für Physik B Condensed Matter* **57**, 233 (1984).
- [4] V. Johny *et al.*, Self-driven nanofluidics at liquid-gas interface, arXiv preprint arXiv:2112.15220 (2021).
- [5] P. Kapitza, Viscosity of liquid helium below the λ -point, *Nature* **141**, 74 (1938).
- [6] N. Bogoliubov, On the theory of superfluidity, *J. Phys* **11**, 23 (1947).
- [7] X. Rojas and J. Davis, Superfluid nanomechanical resonator for quantum nanofluidics, *Physical Review B* **91**, 024503 (2015).
- [8] L. Tisza, Transport phenomena in helium ii, *Nature* **141**, 913 (1938).
- [9] Y. Hao, S. Pang, X. Zhang, and L. Jiang, Quantum-confined superfluid reactions, *Chemical Science* **11**, 10035 (2020).
- [10] A. Ghosh, V. Mukherjee, W. Niedenzu, and G. Kurizki, Are quantum thermodynamic machines better than their classical counterparts?, *The European Physical Journal Special Topics* **227**, 2043 (2019).
- [11] M. Lukin and A. Imamoglu, Nonlinear optics and quantum entanglement of ultraslow single photons, *Physical Review Letters* **84**, 1419 (2000).
- [12] G. Baym and C. J. Pethick, Landau critical velocity in weakly interacting bose gases, *Physical Review A* **86**, 023602 (2012).
- [13] J. P. Reithmaier, G. Sek, A. Löffler, C. Hofmann, S. Kuhn, S. Reitzenstein, L. Keldysh, V. Kulakovskii, T. Reinecke, and A. Forchel, Strong coupling in a single quantum dot–semiconductor microcavity system, *Nature* **432**, 197 (2004).
- [14] H. T. Mebrahtu, I. V. Borzenets, D. E. Liu, H. Zheng, Y. V. Bomze, A. I. Smirnov, H. U. Baranger, and G. Finkelstein, Quantum phase transition in a resonant level coupled to interacting leads, *Nature* **488**, 61 (2012).
- [15] L. Erdős, B. Schlein, and H.-T. Yau, Derivation of the cubic non-linear schrödinger equation from quantum dynamics of many-body systems, *Inventiones mathematicae* **167**, 515 (2007).
- [16] T. Tsuzuki, Nonlinear waves in the pitaeviskii-gross equation, *Journal of Low Temperature Physics* **4**, 441 (1971).
- [17] W. Kohn and D. Sherrington, Two kinds of bosons and bose condensates, *Reviews of Modern Physics* **42**, 1 (1970).
- [18] T. Kanazawa, Non-hermitian bcs-bec crossover of dirac fermions, *Journal of High Energy Physics* **2021**, 1 (2021).
- [19] A. V. Melkikh, Nonlinearity of quantum mechanics and solution of the problem of wave function collapse, *Communications in Theoretical Physics* **64**, 47 (2015).
- [20] R. A. Jishi, *Feynman diagram techniques in condensed matter physics* (Cambridge University Press, 2013).